Research Article

Nanomedicine

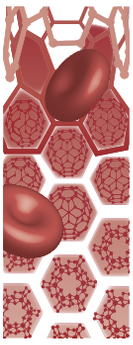

Assay of miRNA in cell samples using enhanced resonance light scattering technique based on self aggregation of magnetic nanoparticles

Qiaoli Yue*,[1], Lixia Tao[1], Yining Hou[1], Cong Zhang[1], Yongping Wang[1], Min Hong[1] & Chen-Zhong Li[1,2]

[1]Department of Chemistry, Liaocheng University, Liaocheng 252059, China

[2]Nanobioengineering/Bioelectronics Laboratory, Department of Biomedical Engineering, Florida International University, Miami, FL 33174, USA

*Author for correspondence: yueqiaoli@yahoo.com

Aims: miRNAs are regarded as potential biomarkers correlated with the development and progression of many diseases. However, it is a challenge to construct a sensitive method to detect them without using time-consuming radioactive labeling or complex amplification strategies. **Methods:** A facile resonance light scattering (RLS) system was developed for the detection of miRNA employing magnetic nanoparticles (MNPs) as RLS probes. MNPs were coated with streptavidin. DNA probes were modified on the surface of MNPs based on the specific interaction of streptavidin and biotin forming MNPs@DNA probes. MNPs@DNA probes dispersed in homogeneous media causing low RLS signal. **Results & conclusion:** miRNA hybridized with DNA probes resulting in the aggregation of MNPs and inducing the enhancement of RLS intensity. miRNAs were determined successfully with limit of detection at 0.9 picomole per liter (pM). The potential clinical application of the present biosensor was also demonstrated by measuring miRNAs in human normal and cancer cells, and human serum samples.

First draft submitted: 28 February 2018; Accepted for publication: 8 May 2018; Published online: 2 October 2018

Keywords: cell samples • magnetic biosensor • miRNA

miRNAs are a class of small, noncoding RNA members that impart post-transcriptional gene regulation through several mechanisms including translational repression and mRNA degradation [1,2]. miRNA sequences have about 22 nucleotides and negatively control about 30% genes expression in post transcription [3]. MiRNAs show their importance in some physiological processes including carcinogenesis and immune system modulation. Furthermore, miRNAs are a relatively new class of biomarkers for diseases such as breast cancer, lung cancer, renal cell carcinomas and glioblastoma [4–6]. miRNA21 (miR-21) is an abundantly expressed miRNA in mammalian cells of multiple types and its expression is enhanced in many disease states including solid tumors, cardiac injury and inflamed tissues [7,8]. PCR-based methodologies are currently popular to detect miRNAs, which show high sensitivity even to 10 fetomole per liter (fM). However, it is necessary to carry out some time-consuming steps including extraction, amplification, calibration, as well as preliminary amplification. In addition, the specificity for primer design may be reduced since miRNAs are short nucleic acids [9]. Hence, some sensitive and advanced monitoring methods need to be improved, because of the small amounts of miRNAs in cells usually present in the nanomolar to femtomolar level [10]. In this work, a facile aptasensor for detection of miR-21 was proposed based on resonance light scattering (RLS) technique.

RLS, produced when the incident beam is close to its molecular absorption, is a kind of elastic light scattering and can be carried out on a common spectrofluorometer [11,12]. It was first proposed by Pasternack *et al.*, to study the aggregation of porphyrin [13,14]. Owing to the distinct advantages of RLS such as high sensitivity, good selectivity, convenient performance and easy detection, RLS was widely used in the designation of bioassembly and

Future Medicine

aggregation processes [15–18] for the application in biochemical [19–21] and pharmaceutical fields [22–24]. More and more studies indicated that RLS method was becoming one of the most popular testing ways in daily application.

Due to the proven biocompatibility and the approval of superparamagnetic iron oxide nanoparticles are the most intensively studied magnetic nanoparticles (MNPs) due to their proven biocompatibility [25,26]. MNPs show crucial advantages in several biomedical applications, such as cellular therapy, tissue repair, targeted drug delivery, MRI and hyperthermia [27]. MNPs possess hydrophobic surfaces with large surface area to volume rations tend to agglomerate [28]. The aggregation of MNPs induces the coupling of magnetic spin moments and generates strong local magnetic fields. Such local magnetic field in homogeneities accelerates the attraction between MNPs and consequently, creating increased aggregation. The switch of self aggregation and dissociation for MNPs were successfully employed for the determination of lysozyme in cancer cell lysates by evaluation of the spin–spin relaxation time T_2 [26].

The aim of this work is to design a novel aptasensor of miR-21, combining the advantages of functionalized MNPs and specific reaction of streptavidin and biotin. In the process, MNPs were used as probes to enhance RLS intensity. The enhancement of RLS derived mainly from miRNA, as well as the self aggregation of MNPs. To confirm the positive effect of self aggregation of MNPs, gold nanoparticles (AuNPs) were also used to construct the similar biosensor. The possible mechanism for the aggregation of MNPs was discussed in detail. The present strategy provided a simple reaction process without any enzymatic amplification. The content of miRNA was analyzed in two human tumor cell lines and one normal cell line, and in human serum samples through this platform, respectively. It may be a potential method to detect miRNA in tumor molecular diagnosis.

Material & methods

Material

MNPs of iron oxide coated with streptavidin were purchased from micromod (Germany), which were cluster-typed with average hydrodynamic particle diameter of 20, 50 and 100 nm, respectively. All DNA and RNA sequences used in the present work were synthesized and purified using HPLC by Sangon Biotechnology Co., Ltd (Shanghai, China), which were listed in Supplementary Table 1. RNase-free water and Tris/Boric Acid/EDTA (TBE) buffer (5×, 225 mM Tris-Boric acid, 50 mM EDTA, pH 7.4) solutions were purchased from Takara Biotechnology Co., Ltd (Dalian, China). DMEM high glucose medium, penicillin, streptomycin and 15% heat-inactivated fetal bovine serum were purchased from Thermo Scientific HyClone (MA, USA). Some common reagents such as sodium acetate, sodium dihydrogen phosphate, acetic acid, hydrochloric acid and other common salts were of analytical grade and obtained from Beijing Chemical Engineering (Beijing, China), which were directly used without further purification. Buffer solutions including tris(hydroxymethyl)-aminomethane, HEPES and MOPS were purchased from Fluka (Buchs, Switzerland). The solutions were prepared using diethy pyrocarbonate (DEPC)-treated water throughout the experiment.

Apparatus

RLS measurements were carried out using an LS-55 spectrophotometer (Perkin Elmer, MA, USA) with a 1 cm-slit sample cell. Absorption spectra were performed on a Lambda 750 spectrophotometer (Perkin Elmer). Digital photos were obtained by Nikon 4500 digital camera (Tokyo, Japan), and transmission electron microscope images were obtained on a JEM-2100 electron microscope operating at 200 kV (JEOL Ltd, Tokyo, Japan).

Preparation of DNA probe modified MNPs

First, DNA probes were modified on the surface of MNPs. Specifically, 0.8 nM probe1 (with sequence of 5′-CTG ATA AGC TAT TT-biotin-3′ as shown in Supplementary Table 1) and probe2 (with sequence of 5′-biotin-TTT TCA ACA TCA GT-3′ as shown in Supplementary Table 1) were added to 0.1 mg ml^{-1} MNPs dispersion, respectively, and then the mixture was diluted to 2.0 ml with 0.01 M phosphate-buffered saline (PBS) buffer solution at pH 7.4. The bonding of DNA probe on the surface of MNPs was based on the fast and specific affinity between biotin and streptavidin. After incubation of 10 min at room temperature (20°C), the MNPs@probe1 and MNPs@probe2 composites formed, respectively, which were used to construct the biosensor of miRNA.

MiRNA detection using MNPs

After DNA probes were linked to MNPs, target miRNA solutions with different concentrations were prepared to be detected. When MNPs@probe1 and MNPs@probe2 dispersions were mixed thoroughly with the addition of

400 µl hybrid solution, the RLS intensity was measured (named RLS_0). A series of miR-21 solutions with different concentrations were added to the mixture of MNPs@probe1 and MNPs@probe2, respectively, and were allowed to be incubated for 20 min at room temperature to form MNPs@probe1-miRNA-MNPs@probe2 complexes. MNPs can aggregate to form big-sized nanoparticles, which lead to the enhancement of RLS signal. The RLS spectra were obtained by scanning the excitation and emission simultaneously ($\Delta\lambda$ = 0 nm) in the wavelength range of 200.0–700.0 nm with the same starting wavelength and scanning speed. The RLS intensity was recorded at the peak of 402 nm. In this process, the slits for excitation and emission monochromator were maintained at 2.5 nm.

MiRNA detection using AuNPs

In this step, Au-thiol chemistry was used to combine AuNPs with S-probes (with sequences listed in Supplementary Table 1). The procedure was reported in our previous work [29]. Specifically, 0.3 nM AuNPs and 1.6 nM S-probes were suspended in a 0.01 M PBS at pH 7.4. The mixture solution was incubated at room temperature for 20 min to build AuNPs@S-probe1 and AuNPs@S-probe2, respectively. Then, 2 M NaCl dissolved in 0.01 M PBS was added to the system to a final concentration of 0.02 M NaCl. The salting process was followed by an overnight incubation at room temperature. AuNPs were allowed to centrifuge to remove excess oligonucleotides and the supernatants were removed. AuNPs modified with S-probes were redispersed in PBS. AuNPs@S-probe1 and AuNPs@S-probe2 dispersions were mixed, and the RLS signals were obtained in the presence and absence of miRNA.

Cell culture & sample preparation

MCF-7 cells (human breast cancer cell lines) and A549 cells (cervical cancer cell lines) were routinely cultured in traditional cell culture dishes using DMEM supplemented with 10% fetal bovine serum, 0.1% penicillin and streptomycin mixture (100 µg ml^{-1}). MCF-10A (mammary epithelial cell lines) were cultured in DMEM/F-12 medium supplemented with 5% horse serum, 0.1% penicillin, 100 µg ml^{-1} streptomycin, 0.5 mg ml^{-1} hydrocortisone, 100 ng ml^{-1} cholera toxin, 10 mg ml^{-1} insulin, 10 ng ml^{-1} EGF and 1% L-glutamine. The cells were cultured in a humidified atmosphere at 37°C with 5% CO_2. Total RNA in MCF-7, A549 and MCF-10A cells was extracted with E.Z.N.A®PF Micro RNA kit (Omega Bio-tek, GA, USA) following the manufacturer's instructions, respectively. Briefly, approximately 8.2×10^5 MCF-7 cells, 6.3×10^6 A549 cells and 1.2×10^6 MCF-10A cells were washed once with phosphate-buffered saline (containing 10 mM PBS, pH 7.4, and 100 mM NaCl) and then were extracted using E.Z.N.A®PF Micro RNA kit. All RNA samples were split into small centrifuge tubes and stored at -80°C until analysis.

Results & discussion

Principle for miRNA detection using MNPs

The newly designed biosensor was mainly based on the use of MNPs as illustrated in Figure 1. DNA probes labeled with biotin can be modified on the surface of MNPs coated with streptavidin through the specific interaction between biotin and streptavidin. DNA probes consisted of two strands (probe1 and probe2, as shown in Supplementary Table 1), which were complementary with target miRNA. First, the biotin-labeled probes were functionalized on MNPs by the specific affinity between biotin and streptavidin named MNPs@probe1 and MNPs@probe2, respectively. In the presence of miR-21, MNPs can form a structure like dumbbell due to the hybridization linkage of DNA probes and aggregated together (Figure 2). The aggregated MNPs can even precipitate at the bottom of the bottle as shown in Figure 2. It was reported that the aggregation of MNPs can produce little local magnetic fields [26]. The little local magnetic fields can accelerate the further agglomeration of MNPs and induce the significant increment of RLS signal. The aggregation of MNPs derived from local magnetic field was confirmed using AuNPs to substitute MNPs, and probes were replaced by S-probes in the sensing system (Figure 1). This method exhibits outstanding sensitivity and selectivity, which can discriminate the target sequence from even single-base mismatched sequences. The result indicates that the proposed biosensor could become a promising miRNA detection method in early clinical diagnostics and biomedical research.

Optimization of conditions

To obtain high sensitivity and selectivity for the detection of miRNA, the experimental conditions were investigated including the size and concentration of MNPs, the concentration of probe DNA, and the temperature and time of reaction.

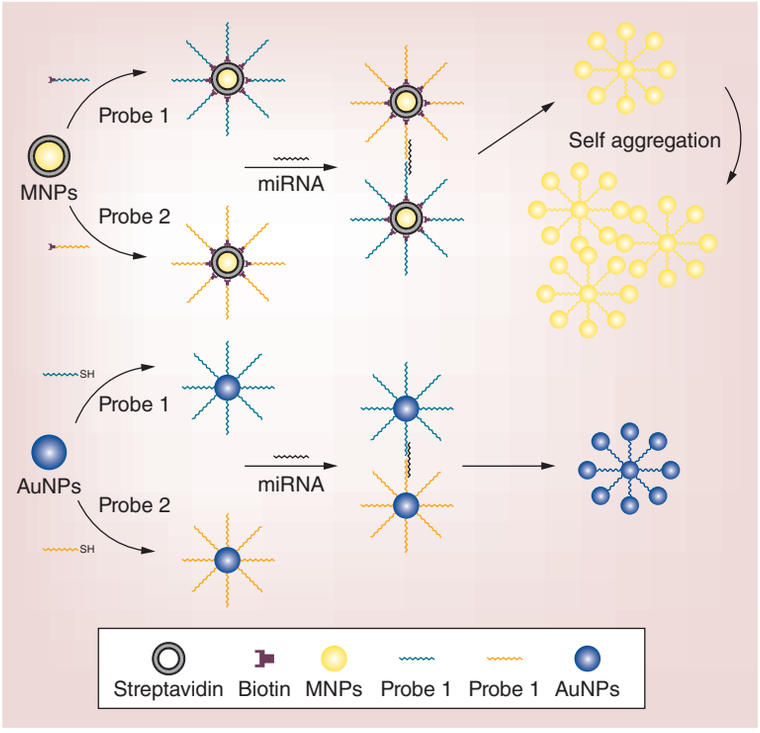

Figure 1. Schematic illustration of miRNA biosensors using magnetic and gold nanoparticles.
AuNPs: Au nanoparticles; MNP: Magnetic nanoparticles.

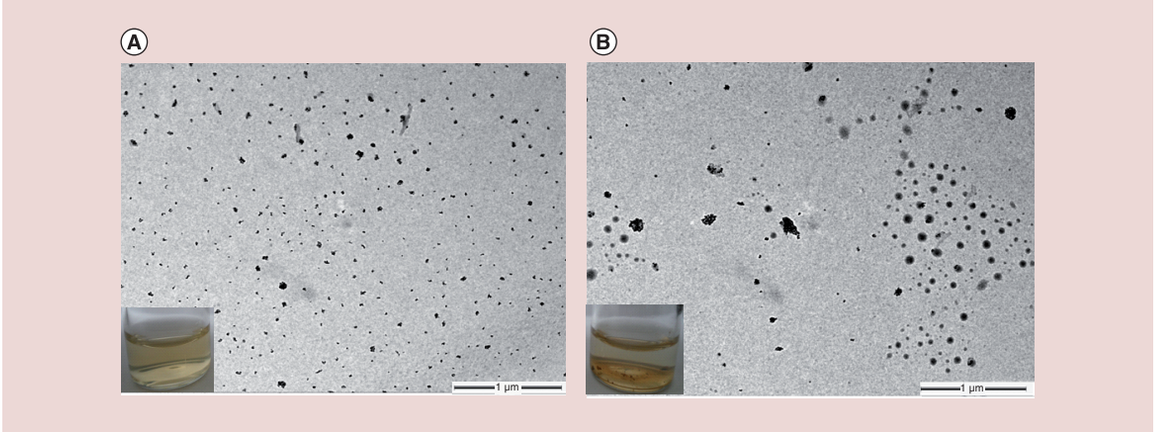

Figure 2. Transmission electron microscope images of magnetic nanoparticles under different conditions.
Transmission electron microscope images for the mixture of MNPs@probe1 and MNPs@probe2 before **(A)** and after **(B)** the addition of miR-21. Inset: responding digital photos for **(A)** and **(B)**. The scale bars were 1.0 μm. Conditions: 50 nm MNPs 0.1 mg ml^{-1}; miR-21 20 nM.

Influence of MNPs

The influences of size and concentration of MNPs on the determination of miRNA were discussed. First, MNPs with different sizes including 20, 50 and 100 nm were employed to test the effect of MNPs size on the detection of miRNA. Then 0.4 nM probes and 0.2 nM MNPs with the size of 20, 50 and 100 nm, respectively, reacted at room temperature for 1 h to build MNPs@probe1 and MNPs@probe2. With the addition of miR-21, RLS intensity of MNPs increased gradually with increasing concentration of miR-21 as shown in Supplementary Figure 1A. It can be seen that three biosensors with 20, 50 and 100 nm sized MNPs were all in good linear relationships between RLS intensity and miRNA concentration. Furthermore, the biosensor with 50 nm-sized MNPs showed highest sensitivity among the tested MNPs (due to the largest slope value).

To discuss the effect of MNPs concentration, 0.01, 0.05, 0.10, 0.20, 0.30 and 0.40 nM MNPs were used to build biosensors, respectively. As illustrated in Supplementary Figure 1B, the increment of RLS intensity (ΔRLS) enhanced with increase of MNPs concentration, and got to a peak at 0.20 nM MNPs. The values of ΔRLS reduced slightly for MNPs concentrations of 0.30 and 0.40 nM. This phenomenon can be explained that although MNPs with higher concentration can generate more assemble of MNPs with same probes and target miRNA, they can still produce higher background. As a result, the ΔRLS values of 0.30 and 0.40 nM MNPs were lower than that of 0.20 nM MNPs. Thus, 0.20 nM MNPs were chosen in the following experiments.

Effect of DNA probes concentration

We investigated the probes concentration at 0.20, 0.40, 0.80, 1.60, 2.40, and 3.00 nM, respectively, by comparison of ΔRLS in the presence and absence of miRNA. As shown in Supplementary Figure 2, it was clear that the value of ΔRLS was dependent strongly on the initial concentration of probes from 0.20 to 1.60 nM. When probes concentration was in the range of 1.60–3.00 nM, ΔRLS changed inconspicuously. Considering both the highest ΔRLS value and the least reagent waste, DNA probes at 1.60 nM were employed as one of the optimum experiment conditions.

Optimization of reaction temperature & time

In order to ensure the efficient combination between MNPs and probes as well as the hybridization of miR-21 and probes, the influences of reaction temperature and time were explored. For the reaction temperature, the system solutions in the presence and absence of miR-21 were incubated at 10, 20, 30 and 40°C, respectively, as shown in Supplementary Figure 3A. It can be found that the ΔRLS value with 150 pM miR-21 was largest at 20°C. Therefore, the room temperature 20°C was used as an optimal condition.

In the presence of miRNA, the hybridization between probes on the surface of MNPs and target miRNA induced the aggregation of MNPs. MiR-21 and the MNPs@probes dispersions were incubated for different time. As demonstrated in Supplementary Figure 3B, an obvious increase of ΔRLS value can be observed from 0 to 10 min, from which it can be concluded that hybridization induced the aggregation of MNPs and resulted in the remarkable enhancement of RLS intensity. ΔRLS increased slightly in the range of 10–20 min. After 20 min, the RLS intensity arrived at a platform, which indicated that probes and target miRNA can react sufficiently within 20 min. In addition, there were two more slopes for the increased part of the curve. It can be deduced that there may be two steps for the aggregation of MNPs. For further detailed information it should be discussed subsequently.

Sensitivity

Target miRNA solutions with a series of different concentrations were measured to investigate the sensitivity of the proposed method. To obtain the best performance of the biosensor, all samples including 0.2 nM 50 nm-sized MNPs connected with 1.60 nM DNA probes and target miRNA with various concentrations were incubated at 20°C for 20 min before carrying out RLS measurements. It can be observed in Figure 3A that RLS peak intensities increased along with the increased concentration of target miRNA. Figure 3B showed the variation of the peak intensity as a function of the concentration of target miRNA. The relationship of ΔRLS and the concentration of miR-21 was in a good linearity with the concentration range of 3.0–300 pM (R^2 = 0.9971). All the RLS measurements were carried out three-times independently. According to the recent recommendation of International Union of Pure and Applied Chemistry (IUPAC), the limit of detection can be obtained as 0.9 pM from the equation of 3.29 S_B/m, where S_B and m were the standard deviation of the blank and slope of the calibration graph, respectively. Notably, the sensitivity of the proposed biosensor was superior to those of fluorescence assays using circular exponential amplification [30], electrochemical strategies using recycling amplification [31] and PCR-based approaches using recombinase polymerase amplification [32] as well. The comparison of the present assay with other methods was illustrated in Supplementary Table 2 in detail. The proposed biosensor showing significant improvement in sensitivity can mainly be attributed to the aggregation of MNPs due to the interaction of DNA probes and miR-21 and sensitive RLS detection as well. It was proved that from the above results the biosensor fabricated in this work can ensure picomolar level detection of miRNA.

To signify the signal amplification of MNPs, we also studied detection sensitivity for miR-21 using AuNPs. As statemented in Material and Methods, a series of miR-21 stock solutions with different concentrations was added to AuNPs@S-probes system, respectively, which also induced the enhancement of RLS intensity. It was worthy to note that a linear relationship between ΔRLS and the concentration of miR-21 was also obtained in Figure 4. It

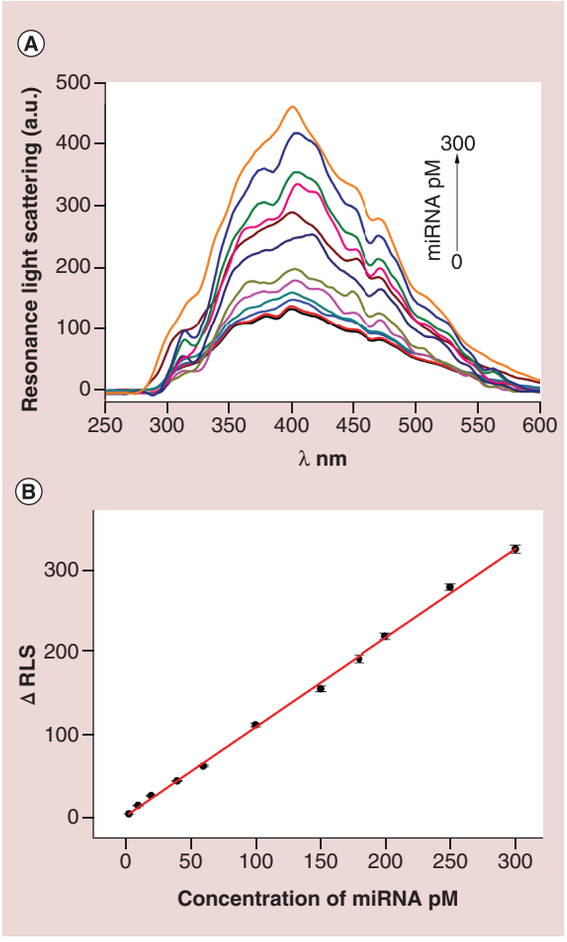

Figure 3. Sensitivity test results for miR-21 detection. Resonance light scattering spectra **(A)** and responding linear relationship **(B)** between increment of resonance light scattering intensity value and the concentration of miR-21 within the range of 3.0 to 300 pM.

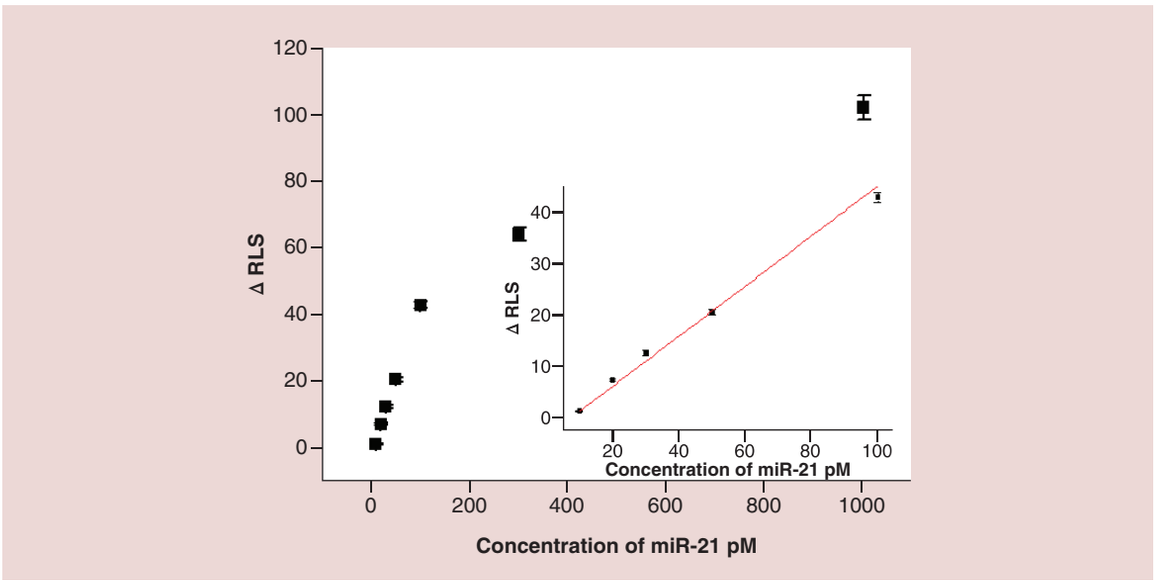

Figure 4. Response of increment of resonance light scattering intensity to miR-21 concentration ranging from 10 pM to 1.0 nM using gold nanoparticles as resonance light scattering probe. Inset: The resulting linear relationship between increment of resonance light scattering intensity and miR-21 concentration in the range of 10 to 100 pM.

was observed that ΔRLS increased with increasing concentration of miR-21 from 10.0 pM to 10.0 nM. The linear equation was ΔRLS = 0.487*C* - 3.51 in the concentration range from 10.0 to 100.0 pM with a linear correlation of *R* = 0.9949, where *C* was the concentration of miR-21. By comparison, it was obvious that the slope of the linearity using AuNPs was lower and the linear concentration range was narrower than those of MNPs, respectively. It can be deduced that the detection sensitivity for AuNPs system was lower than that of MNPs, though the linear curves were good enough to detect miR-21 for the two biosensors constructed using AuNPs and MNPs as RLS probes, respectively. It can be attributed to the aggregation of MNPs derived from aggregation-induced local magnetic fields.

Specificity

The biosensor not only provided improved detection sensitivity but also afforded high selectivity for target miR-21 detection. To further evaluate the specificity of the proposed method, five kinds of miRNA sequences were employed, including perfect complementary target miR-21, single-base mismatched miR-21 named miR-21a, two-base mismatched miR-21 named miR-21b, four-base mismatched miR-21 named miR-21c and noncomplementary sequence of miR-141, which were listed in Supplementary Table 1. ΔRLS values for all tested miRNA sequences were obtained with results shown in Figure 5A. It was found that the RLS signal was close to the blank for nonhomologous miRNA, miR-141. Moreover, it can be observed that miR-21a with single-base mismatch at the 3′ terminus (with the bold letter shown in Supplementary Table 1) also did not cause any interference. In addition, the specificity experiment was also executed with different incubation time (Figure 5B). It was suggested that the value of ΔRLS for miR-21 was significantly higher than those of other species. The slope of every curve in the range of 0–10 min varied from that of 10–15 min, which was the further evidence for the two-step aggregation of MNPs. In addition, the incubation time of 15 min was enough for miRNA species except miR-21. It can be concluded that the platform has a splendid specificity that is potential to give out a specific detection signal from the complex extractions of tumor cells.

Application

Since miR-21 is a potential cancer biomarker, which has been identified with elevated expression levels in numerous tumor tissues, such as breast, liver, ovarian, pancreatic and brain, in comparison to their normal counterparts, miR-21 was usually detected in human cancer cells and human serum samples. Herein, to demonstrate the capability of the fabricated biosensor for miRNA in real sample analysis, miR-21 in total RNA extracts of human cell samples were investigated. Two human cancer cell lines (A549 and MCF-7) with high miR-21 expression levels and one normal cell line (MCF-10a) were selected to investigate the capacities for detection of cell extractions using the developed strategy (Figure 6). All cell samples set as about 10^6 cells for each group were processed by a total RNA extraction kit after cell counting as illustrated in Material and Methods. It can be found that ΔRLS values of tumor cells were obviously stronger than that of normal cells. For cancer cells, miR-21 expression level was higher in A549 cell line. It indicated that there was distinct miR-21 expression difference between human cancer cells and normal cells, which was in a good agreement with the data reported previously [33].

The accuracy of the method was also determined by measuring the recovery of known amounts of miR-21 spiked into the cellular extract of MCF-7 cell and human serum samples. As shown in Supplementary Table 3, the recovery was found to be from 95.6 to 107.8% for 5, 10 and 20 pM of miR-21 spiked per well. Two human serum samples (obtained from the People's Hospital of Liaocheng, China) were also prepared by addition of miR-21 standard solutions. Various concentrations of miR-21 were added into the 20-fold diluted healthy human serum samples. Supplementary Table 4 showed the recovery test of spiked miR-21 in serum. It can be observed that the recovery values varied from 98.89 to 103.4% and RSD was <3.5%. The studies demonstrated the feasibility of the developed approach in the detection of miR-21 directly from a cellular extract and serum samples.

Conclusion

In summary, a specific RLS method was developed for the assay of sub-picomolar level of miRNA based on MNPs enhancement. It was constructed by combining both advantages of aptamer and MNPs. Biotin labeled DNA probes can be modified on the surface of streptavidin coated MNPs. Target miRNA can induce the aggregation of MNPs owing to the partial hybridization of miRNA and DNA probes. The aggregation of MNPs may derive from two processes, in which one is the reaction of miRNA and DNA probes and the other is self aggregation of MNPs based on many local magnetic fields. The aggregation of MNPs can induce the enhancement of RLS signal, and therefore

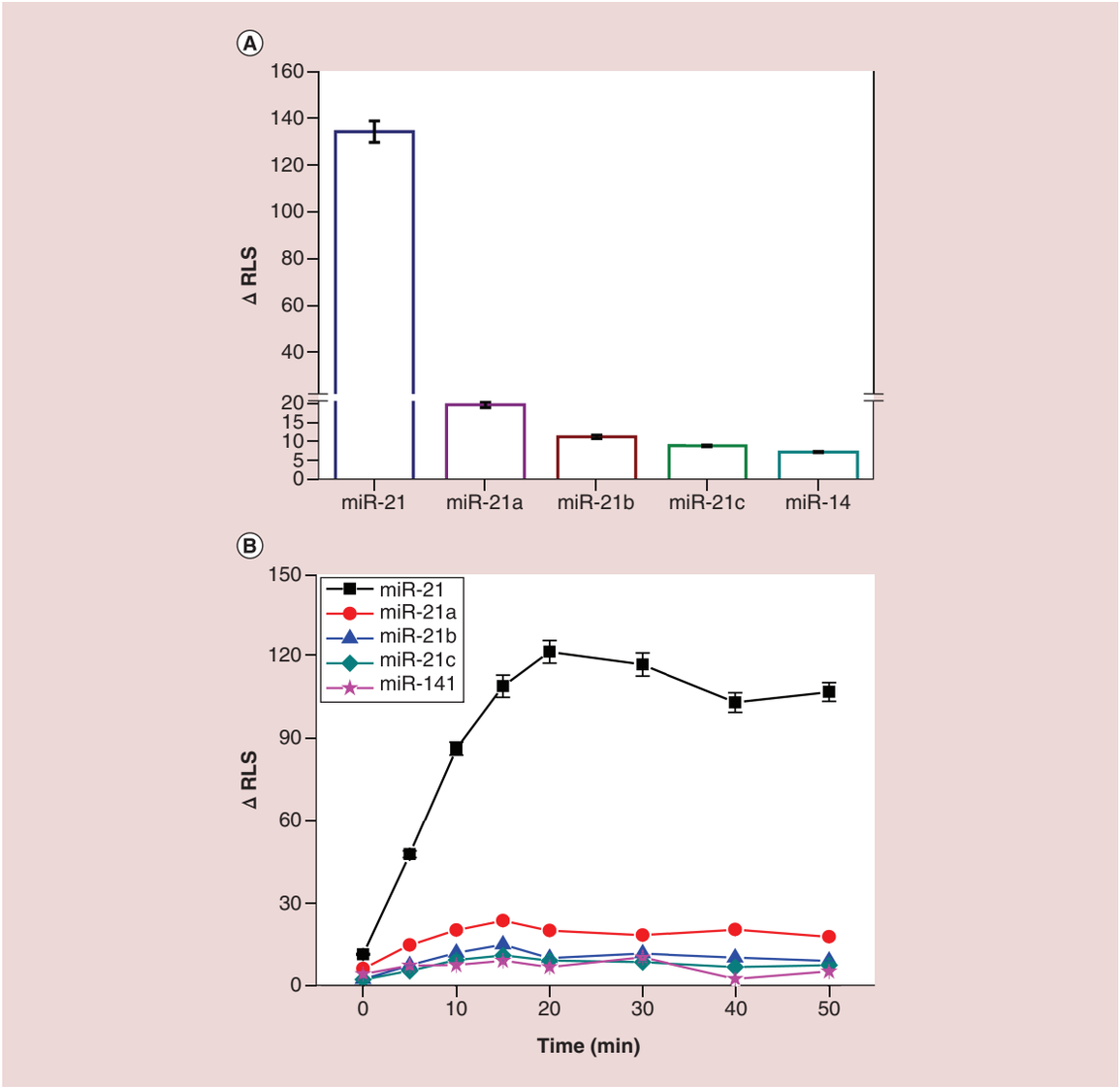

Figure 5. Selectivity test results for miR-21 determination. Resonance light scattering change upon the addition of different miRNA sequences **(A)** and response of increment of resonance light scattering intensity value to reaction time in the presence of various miRNA species **(B)**.

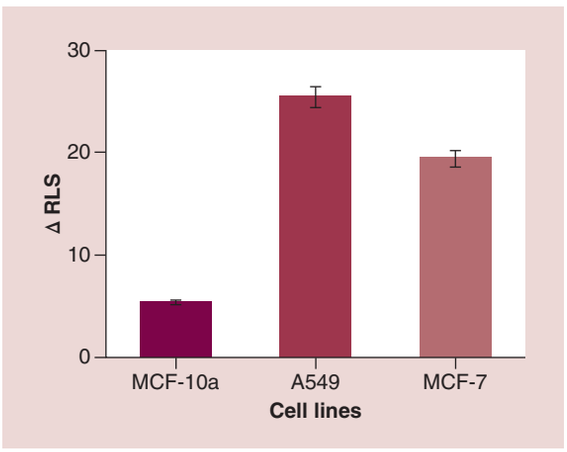

Figure 6. Comparison of miR-21 expression level in human normal cell lines of MCF-10a and tumor cell lines of A549 and MCF-7.
RLS: Resonance light scattering.

the content of target miRNA was detected. The results showed that the sensitivity for miRNA detection using MNPs was higher than that of AuNPs. The aptasensor demonstrated high sensitivity with a LOD of miRNA at 0.9 pM in buffer solutions under optimum conditions. It also showed high specificity for discriminating differences between miRNA family members even the single-base mismatched sequences. Moreover, the project can easily be extended to build a series of systems by simply changing the functional probes on the surface of MNPs (as shown in Figure 1). The DNA probes can be selected according to specific miRNA in the unimolecular DNA template to quantify different kinds of miRNA (biomarkers) with high sensitivity in cells or serum samples. It may supply valuable information for biomedical research and clinical early diagnosis.

Summary points

- MiRNAs are regarded as potential biomarkers correlated with many diseases.
- It is a challenge to construct a sensitive method for miRNAs assay without using time-consuming radioactive labeling or complex amplification strategies.
- A facile resonance light scattering (RLS) system was developed for the detection of miRNA employing magnetic nanoparticles (MNPs) as RLS probes.
- Target miRNA was determined with a dynamic range from 3.0 to 300 pM, and the limit of detection was 0.9 pM.
- The aptasensor showed high specificity for discriminating differences between miRNA family members even the single-base mismatched sequences.
- The project may supply valuable information for biomedical research and clinical early diagnosis.

Supplementary data

To view the supplementary data that accompany this paper please visit the journal website at: www.futuremedicine.com/doi/full/10.2217/nmm-2018-0066

Financial & competing interests disclosure

This work was financially supported by Natural Science Foundation of China (91543206), Natural Science Foundation (ZR2014BQ017, ZR2015BM024 and 2013SJGZ07) and Tai-Shan Scholar Research Fund of Shandong Province and research foundation of Liaocheng University. The authors have no other relevant affiliations or financialinvolvement with any organization or entity with a financial interest in or financial conflict with the subject matter or materials discussed in the manuscript apart from those disclosed.

No writing assistance was utilized in the production of this manuscript.

References

1. Ambros V. The functions of animal microRNAs. *Nature* 431, 350–355 (2004).
2. Murugaiyan G, Cunha APd, Ajay AK *et al.* MicroRNA-21 promotes Th17 differentiation and mediates experimental autoimmune encephalomyelitis. *J. Clin. Invest.* 125, 1069–1080 (2015).
3. Bartel DP. MicroRNAs: genomics, biogenesis, mechanism, and function. *Cell* 116, 281–297 (2004).
4. Wotschofsky Z, Liep J, Meyer H-A *et al.* Identification of metastamirs as metastasis-associated micrornas in clear cell renal cell carcinomas. *Int. J. Biol. Sci.* 8, 1363–1374 (2012).
5. Lawler SE. MicroRNA functions and potential clinical utility in glioblastoma. *Curr. Signal Transduction Ther.* 8, 36–44 (2013).
6. Zhang J, Fu Y, Mei YP *et al.* Fluorescent metal nanoshell probe to detect single miRNA in lung cancer cell. *Anal. Chem.* 82, 4464–4471 (2010).
7. Landgraf P, Rusu M, Sheridan R *et al.* A mammalian microRNA expression atlas based on small RNA library sequencing. *Cell* 129, 1401–1414 (2007).
8. Volinia S, Calin GA, Liu C-G *et al.* A microRNA expression signature of human solid tumors defines cancer gene targets. *Proc. Natl Acad. Sci. USA* 103, 2257–2261 (2006).
9. Hlousek L, Voronov S, Diankov V *et al.* Automated high multiplex qPCR platform for simultaneous detection and quantification of multiple nucleic acid targets. *BioTechnique* 52, 316–324 (2012).
10. Mitchell PS, Parkin RK, Kroh EM *et al.* Circulating microRNAs as stable blood-based markers for cancer detection. *Proc. Natl Acad. Sci. USA* 105, 10513–10518 (2008).
11. Anglister J, Steinberg IZ. Resonance Rayleigh scattering of cyanine dyes in solution. *J. Chem. Phys.* 78, 5358–5368 (1983).

12. Collings PJ, Gibbs EJ, Starr TE *et al.* Resonance light scattering and its application in determining the size, shape, and aggregation number for supramolecular assemblies of chromophores. *J. Phys. Chem. B.* 103, 8474–8481 (1999).
13. Pasternack RF, Bustamante C, Collings PJ *et al.* Porphyrin assemblies on DNA as studied by a resonance light-scattering technique. *J. Am. Chem. Soc.* 115, 5393–5399 (1993).
14. Pasternack RF, Collings PJ. Resonance light scattering: a new technique for studying chromophore aggregation. *Science* 269, 935–939 (1995).
15. Ribó JM, Crusats J, Sagués F *et al.* Chiral sign induction by vortices during the formation of mesophases in stirred solutions. *Science* 292, 2063–2066 (2001).
16. Kano K, Fukuda K, Wakami H, Nishiyabu R, Pasternack RF. Factors influencing self-aggregation tendencies of cationic porphyrins in aqueous solution. *J. Am. Chem. Soc.* 122, 7494–7502 (2000).
17. Micali N, Mallamace F, Romeo A *et al.* Mesoscopic structure of meso-tetrakis(4-sulfonatophenyl)porphine J-aggregates. *J. Phys. Chem. B.* 104, 5897–5904 (2000).
18. Choi MY, Pollard JA, Webb MA, Mchale JL. Counterion dependent excitonic spectra of tetra(p-carboxyphenyl)porphyrin aggregates in acidic aqueous solution. *J. Am. Chem. Soc.* 125, 810–820 (2003).
19. Huang CZ, Li KA, Tong SY. Determination of nucleic acids by a resonance light-scattering technique with a,b,g,d-tetrakis[4-(trimethylammoniumyl) phenyl]porphine. *Anal. Chem.* 68, 2259–2263 (1996).
20. Chen ZG, Song TH, Peng YR *et al.* A new way to detect the interaction of DNA and anticancer drugs based on the decreased resonance light scattering signal and its potential application. *Analyst* 136, 3927–3933 (2011).
21. Zheng J, Cheng GF, He PG *et al.* An aptamer-based assay for thrombin via structure switch based on gold nanoparticles and magnetic nanoparticles. *Talanta* 80, 1868–1872 (2010).
22. Liu S, Luo H, Li N *et al.* Resonance Rayleigh scattering study of the interaction of heparin with some basic diphenyl naphthylmethane dyes. *Anal. Chem.* 73, 3907–3914 (2001).
23. Feng P, Shu WQ, Huang CZ, Li YF. Total internal reflected resonance light scattering determination of chlortetracycline in body fluid with the complex cation of chlortetracycline-europium-trioctyl phosphine oxide at the water/tetrachloromethane interface. *Anal. Chem.* 73, 4307–4312 (2001).
24. Chen ZG, Song TH, Wang SB *et al.* Screening DNA-targeted anticancer drug *in vitro* based on the drug-conjugated DNA by resonance light scattering technique. *Biosens. Bioelectron.* 25, 1947–1952 (2010).
25. Lin MM, Kim DK, El Haj AJ, Dobson J. Development of superparamagnetic iron oxide nanoparticles (SPIONS) for translation to clinical applications. *IEEE. Trans. Nanobioscience* 7, 298–305 (2008).
26. Bamrungsap S, Shukoor MI, Chen T, Sefah K, Tan W. Detection of lysozyme magnetic relaxation switches based on aptamer-functionalized superparamagnetic nanoparticles. *Anal. Chem.* 83, 7795–7799 (2011).
27. Trana N, Webster TJ. Magnetic nanoparticles: biomedical applications and challenges. *J. Mater. Chem.* 20, 8760–8767 (2010).
28. Gupta AK, Gupta M. Synthesis and surface engineering of iron oxide nanoparticles for biomedical applications. *Biomaterials* 26, 3995–4021 (2005).
29. Yue QL, Shen TF, Wang CN *et al.* Construction of a controllable Forster resonance energy transfer system based on G-quadruplex for DNA sensing. *Biosens. Bioelectron.* 40, 75–81 (2013).
30. Dong HF, Meng XD, Dai WH *et al.* Highly sensitive and selective microRNA detection based on DNAbio-bar-code and enzyme-assisted strand cycle exponential signal amplification. *Anal. Chem.* 87, 4334–4340 (2015).
31. Zhu D, Liu W, Zhao DX *et al.* Label-free electrochemical sensing platform for microRNA-21 detection using thionine and gold nanoparticles co-functionalized MoS_2 nanosheet. *ACS Appl. Mater. Interfaces* 9, 35597–35603 (2017).
32. Wee EJH, Trau M. Simple isothermal strategy for multiplexed, rapid, sensitive, and accurate miRNA detection. *ACS Sens.* 1, 670–675 (2016).
33. Lu J, Getz G, Miska EA *et al.* MicroRNA expression profiles classify human cancers. *Nature* 435, 834–838 (2005).